RESEARCH ARTICLE

Expanding the clinical and phenotypic heterogeneity associated with biallelic variants in *ACO2*

Patrick R. Blackburn[1] [iD], Matthew J. Schultz[1], Carrie A. Lahner[1], Dong Li[2], Elizabeth Bhoj[2], Laura J. Fisher[3], Deborah L. Renaud[4], Amy Kenney[5], Niema Ibrahim[6], Mais Hashem[6], Mohammed Zain Seidahmed[7], Linda Hasadsri[1], Samantha A. Schrier Vergano[5,8], Fowzan S. Alkuraya[6,9] [iD] & Brendan C. Lanpher[3]

[1]Department of Laboratory Medicine and Pathology, Mayo Clinic, Rochester, Minnesota
[2]Center for Applied Genomics, Children's Hospital of Philadelphia, Philadelphia, Pennsylvania
[3]Department of Clinical Genomics, Mayo Clinic, Rochester, Minnesota
[4]Departments of Neurology and Pediatrics, Mayo Clinic, Rochester, Minnesota
[5]Division of Medical Genetics and Metabolism, Children's Hospital of The King's Daughters, Norfolk, Virginia
[6]Department of Genetics, King Faisal Specialist Hospital and Research Center, Riyadh, Saudi Arabia
[7]Division of Neonatology, Department of Pediatrics, Security Forces Hospital, Riyadh, Saudi Arabia
[8]Department of Pediatrics, Eastern Virginia Medical School, Norfolk, Virginia
[9]Department of Anatomy and Cell Biology, College of Medicine, Alfaisal University, Riyadh, Saudi Arabia

Abstract

Objective: We describe the clinical characteristics and genetic etiology of several new cases within the ACO2-related disease spectrum. Mitochondrial aconitase (ACO2) is a nuclear-encoded tricarboxylic acid cycle enzyme. Homozygous pathogenic missense variants in the *ACO2* gene were initially associated with infantile degeneration of the cerebrum, cerebellum, and retina, resulting in profound intellectual and developmental disability and early death. Subsequent studies have identified a range of homozygous and compound heterozygous pathogenic missense, nonsense, frameshift, and splice-site *ACO2* variants in patients with a spectrum of clinical manifestations and disease severities. **Methods**: We describe a cohort of five novel patients with biallelic pathogenic variants in *ACO2*. We review the clinical histories of these patients as well as the molecular and functional characterization of the associated *ACO2* variants and compare with those described previously in the literature. **Results**: Two siblings with relatively mild symptoms presented with episodic ataxia, mild developmental delays, severe dysarthria, and behavioral abnormalities including hyperactivity and depressive symptoms with generalized anxiety. One patient presented with the classic form with cerebellar hypoplasia, ataxia, seizures, optic atrophy, and retinitis pigmentosa. Another unrelated patient presented with ataxia but developed severe progressive spastic quadriplegia. Another patient demonstrated a spinal muscular atrophy-like presentation with severe neonatal hypotonia, diminished reflexes, and poor respiratory drive, leading to ventilator dependence until death at the age of 9 months. **Interpretation**: In this study, we highlight the importance of recognizing milder forms of the disorder, which may escape detection due to atypical disease presentation.

Introduction

ACO2 encodes mitochondrial aconitase 2 (MIM: 100850), an iron-dependent tricarboxylic acid (TCA) cycle enzyme that catalyzes the reversible isomerization of citrate to isocitrate. ACO2 is ubiquitously expressed and has been

shown to be important in mitochondrial DNA maintenance.[1] Both homozygous or compound heterozygous missense and frameshift variants in *ACO2* are associated with infantile cerebellar-retinal degeneration (ICRD, MIM: 614559) and optic atrophy 9 (MIM: 616289). The first reported cases of ICRD were in two consanguineous

families with infantile-onset optic atrophy, cerebellar atrophy, hearing loss, and profound global developmental delay.[2] Subsequent studies in additional families noted the core symptoms of ataxia and developmental delay, but not all patients had optic nerve involvement and the severity of the clinical symptoms varied widely.[3,4] Some mild cases have been described in association with nystagmus, abnormal pursuit, cogwheel saccades, head bobbing, dysarthria, and delayed psychomotor development. Two recent publications also described individuals with *ACO2* variants with microcephaly and spastic paraplegia as the major presenting feature, suggesting that the phenotypic spectrum of this disorder is still being defined.[5–7]

To date there have been 34 unique disease associated variants in *ACO2* described in 26 individuals/families detected through untargeted sequencing and subsequent familial testing. Despite the central role of ACO2 in the TCA cycle, patients have not demonstrated obvious biochemical derangements. Additionally, residual enzymatic activity does not fully correlate with the severity of clinical symptoms. This adds an additional layer of diagnostic complexity when variants of uncertain significance are identified in *ACO2*. Here, we present five new cases that significantly expand the mutational and clinical spectrum for this disorder and highlight the importance of recognizing attenuated forms of the disorder which may escape detection. We propose unifying the diverse clinical presentations under the umbrella of ACO2-related disorders.

Methods

Patients

Our cohort consists of five newly described cases with a molecular diagnosis of *ACO2* deficiency. The presentation and clinical course for each patient is summarized in Table 1. Two of these patients (P4 and P5) were briefly described in a large clinical exome sequencing (CES) study of >2200 Saudi families (cases REQ18-2038 and 17-6359, respectively), but are reported in detail here.[8] Individuals were also identified and enrolled in the current study using GeneMatcher[9] (Clinical data were retrospectively collected by each clinician participating in the study. The study was approved by our local institutional review board and in accordance with the Declaration of Helsinki. In addition, written informed consent was obtained to publish subject photographs.

Genetic analyses

All variants are reported based on NCBI reference sequences NM_001098.2 (Protein: NP_001089.1). Clinical trio whole-exome sequencing (WES, Mayo Clinic Laboratories, Rochester, MN) was performed and revealed two

compound heterozygous variants of uncertain significance, c.2153T>C:p.(Ile718Thr) and c.2050C>T:p.(Arg684Trp), in *ACO2* in P1. These variants were confirmed by familial mutation testing (Sanger sequencing confirmation) in P2 and established mode of inheritance in both parents. Similarly, research WES[10] was performed in P3 who was found to carry two novel variants, c.719G>A: p.(Gly240Asp) and c.433-2_433-1delinsCT. Confirmatory sequencing to determine inheritance could only be performed for this patient's mother (father deceased). Singleton clinical WES was performed in P4 and P5 as previously described and identified two private homozygous variants in *ACO2* c.1187C>T: p.(Ser396Leu) and c.2338_2339delCA: p.(Gln780ValfsTer63), respectively.[11] Familial segregation was confirmed via Sanger sequencing in both individuals.

In silico predictions for nonsynonymous variants were performed using Variant Score Ranker (http://vsranker.broadinstitute.org/).[12] Simulations were performed using a homology model (PDB: 1b0j.1.A) of human mitochondrial aconitate hydratase (Q99798) from the SWISS-MODEL Repository (SMR) and generated by the SWISS-MODEL homology modeling pipeline.[13] DynaMut was used to analyze and visualize changes in protein dynamics and stability resulting from vibrational entropy changes caused by missense mutations in ACO2 using normal-mode analysis (http://biosig.unimelb.edu.au/dynamut/).[14] Variant allele frequencies were evaluated in gnomAD (https://gnomad.broadinstitute.org/).[15] Missense Tolerance Ratio (MTR) scores and graphs were generated using MTR-Viewer (http://biosig.unimelb.edu.au/mtr-viewer/).[16] Protein and transcript diagrams were generated using ProteinPaint (https://proteinpaint.stjude.org/).[17]

Results

Clinical reports

In this study, we describe two brothers (P1 and P2), currently 12 and 15 years of age, who presented initially with ataxia at 12 and 20 months, respectively, in the setting of intercurrent febrile illnesses (Fig. 1A). Their ataxia resolved and recurred episodically, correlating to routine viral infections. Both brothers have mild developmental delays, severe expressive speech disorder with dysarthria, behavioral abnormalities including attention deficit hyperactivity disorder (ADHD), depressive symptoms with generalized anxiety, and impaired fine motor skills. Neither brother had significant dysmorphic features (Fig. 1B). Additionally, both brothers were initially thought to have susceptibility to infections but workup for suspected immune deficiencies was unrevealing. Both brothers have received monthly intravenous immunoglobulin (IVIg), however, which may have led to clinical improvement.

Table 1. Table summarizing clinical characteristics of patients with ACO2-related disorders identified in this cohort.

Gene altered	Case 1 ACO2		Case 2 ACO2		Case 3 ACO2		Case 4 ACO2		Case 5 ACO2	
Variants observed	NM_001098.2 c.2050C>T p.(Arg684Trp)	c.2153T>C p.(Ile718Thr)	NM_001098.2 c.2050C>T p.(Arg684Trp)	c.2153T>C p.(Ile718Thr)	NM_001098.2 c.719G>A p.(Gly240Asp)	c.433-2_433-1 delinsCT Abolishes splice site	NM_001098.2 c.1187C>T p.(Ser396Leu)	c.1187C>T p.(Ser396Leu)	NM_001098.2 c.2338_2339delCA p.Gln780ValfsTer63	c.2338_233 9delCA p.Gln780 ValfsTer63
Mode of inheritance	Maternal	Paternal	Maternal	Paternal	N/A (Father deceased)	Maternal	Maternal	Paternal	Maternal	Paternal
gnomAD allele frequency	0.00007481	N/R	0.00007481	N/R	0.000007953	N/R	N/R		N/R	N/R
gnomAD hom	0	N/R	0	N/R	0	N/R	N/R		N/R	N/R
Method of mutation detection	Exome sequencing (trio)		Familial mutation testing (Sanger sequencing)		Exome sequencing (singleton)		Exome sequencing (singleton)		Exome sequencing (singleton)	
Gender	Male		Male		Female		Male		Female	
Age at last investigation	12		15		26		9 months (deceased)		11 years	
Consanguinity	No		No		No		Yes (parents first cousins)		Presumed (unknown)	
Siblings	Brother (affected)		Brother (affected)		Two older half-siblings		None		None	
Birth										
Pre- and postnatal history, gestational week	During pregnancy mother had hyperemesis and failed glucose tolerance test; possible early placenta previa which resolved, delivered by C-section full term (38 weeks)		Full term (week unknown)		Premature (week unknown)		Delivered normally at term to a 27-year-old primigravida mother, Apgar scores were 9 and 10 at 1 and 5 min, respectively, admitted to NICU at the age of 2 h because of generalized cyanosis		Full-term uneventful pregnancy, NSVD,	
Birth weight (grams/SD)	4366 g (70th %-centile)		4196 g (60th %-centile)		1800 g (<1 %-centile)		2850 g (10th %-centile)		N/A	
Birth length (cm/SD)	N/A		N/A		48 cm (5th %-centile)		50 cm (15th %-centile)		N/A	
Birth head circumference (cm/SD)	N/A		N/A		N/A		33 cm (2nd %-centile)		N/A	
Growth										
Growth failure?	No		No		No		N/R		Yes	
Height at age last investigation (cm/SD)	150.5 cm (03/2017) (50th %-centile)		166.4 cm (11/2017) (30th %-centile)		Not measured (wheelchair)		N/R		Not measured (wheelchair)	
Weight at age last investigation (kg/SD)	46.3 kg (03/2017) (70th %-centile)		66.5 kg (11/2017) (80th %-centile)		71 kg in 1/2017 (80th %-centile)		N/R		22.2 kg in 5/2019 (11 years) (<1 %-centile)	
Head circumference at age last investigation (cm/SD)	N/A		N/A		57 cm (1/2017) (90th %-centile)		N/R		46 cm in 3/2012 (4 years) (1st %-centile)	
CNS										
Degree of developmental delay or ID	Mild global developmental delay		Mild developmental delay, a couple grade levels behind chronological age, he has not had any permanent regression		Moderate–severe		Severe		Severe	

(Continued)

Table 1 Continued.

Gene altered	Case 1 ACO2	Case 2 ACO2	Case 3 ACO2	Case 4 ACO2	Case 5 ACO2
Age of walking	2 years and 3 months, unsteady	18 months	Never walked	Never walked	Never walked
Age of first words	4 words at 19 months	5 words at 22 months	12 years 4–5 words	No words	No words
Speech abilities	Patient has a severe speech sound disorder; dysarthric, uses phrase speech appropriately, normal prosody, tone, and volume, increased speech latency; received speech therapy starting at 2 years	Patient has a severe speech sound disorder with characteristics of dysarthria; received speech therapy starting at age 3		No words	No words
Seizures	Starring spells suggestive of seizures	Absent	Present	Present	Present
EEG anomalies	EEG performed in 2016 (age 9). The short-term video EEG showed frontally predominant, generalized spike-wave fragments which could be consistent with a generalized seizure disorder. Dysrhythmia grade 3 generalized atypical spike and wave discharges (awake and asleep). The short-term video EEG recording during wakefulness contained 9 Hz activity over the posterior head regions. During wakefulness, rare fragments of frontally predominant spike and wave were seen lasting <1 s. No additional activation occurred with hyperventilation or photic stimulation. During the recording, the patient fell asleep spontaneously. During sleep, there was somewhat increased activation of frontally predominant spike-wave fragments, with at times some polyspike discharges.	EEG in 2006 and 2007 were normal	Fragments of generalized, poorly formed low-voltage bifrontally predominant spike and wave discharges; possible absent posterior dominant rhythm (age 26)	EEG revealed gross abnormality consistent with multifocal epilepsy; seizures controlled with clonazepam	First seizure at age 3 months and has been persistent with at least one seizure per week since then despite being on 3 AEDs (Levetiracetam, topiramate, and lamotrigine)

(Continued)

Table 1 Continued.

Gene altered	Case 1 ACO2	Case 2 ACO2	Case 3 ACO2	Case 4 ACO2	Case 5 ACO2
Respiratory	N/R	N/R	N/R	Patient had poor respiratory drive, CO_2 retention with respiratory acidosis; due to central apnea he was given ventilatory support and remained on support until death at the age of 9 months	N/A
Motor skills	Able to walk without assistance, motor testing-revealed severely impaired fine-motor dexterity with both hands; visual-motor integration (i.e., copying geometric shapes) was also impaired	Able to walk without assistance, no abnormal motor movements noted	Pulled to stand, does not walk	SMA-like presentation	Severely impaired
Hypotonia/hypertonia	Not noted	During episodes some decreased tone and facial droop (paralysis) with an unsteady gait noted	Not noted	Severe neonatal hypotonia	Severe hypertonia and progressive spastic quadriplegia
Tendon reflexes	Deep tendon reflexes normal and symmetric	Deep tendon reflexes normal and symmetric	Hyporeflexic throughout	Diminished reflexes	Exaggerated
Ataxia	Present	Present	Present	N/R	N/A
Ataxia exacerbated by intercurrent illness?	Present	Present	Unknown	N/R	N/A
Brain imaging done: yes/no; age	MRI (2 years and 3 months) of the brain revealed slightly small pons and superior cerebellar vermis for age but did not show abnormalities of the corpus callosum. MRI of the spine was normal and there was no evidence of tethered cord	MRI at 6 years of age; midbrain, pons, and middle cerebellar peduncles are small in size for his age. The cerebellar hemispheres are basically normal, although the superior cerebellar vermis may be slightly small in size. The corpus callosum appears normal	Brain MRI showed mild cerebellar atrophy (done at age 14 and 16); Brain CT at age 18, same findings	Brain MRI showed dilatation of the ventricles and prominent subarachnoid spaces, thinning of the corpus callosum, hypoplastic cerebellar vermis, and hypoplastic pons	Global hypomyelination (<4 years, exact date unknown)
Cerebellar atrophy	None	None	Present	Present	In the process of retrieving original images to re-evaluate
Behavioral anomalies	ADHD combined type	Depressive symptoms along with generalized anxiety	None significant	N/A	Hyperactivity on clonidine
Organs Retinal dystrophy (age at diagnosis)	None	None	Retinitis pigmentosa at age 12–13	Present	Not assessed but has absent visually-evoked potential (VEP) indicating severely impaired vision

(Continued)

Table 1 Continued.

Gene altered	Case 1 ACO2	Case 2 ACO2	Case 3 ACO2	Case 4 ACO2	Case 5 ACO2
Optic atrophy	None	None	Present	Present	N/A
Abnormal saccades	Present	Present	Present	N/R	N/A
Ophthalmology	Abnormal eye movements in infancy with occasional large horizontal head thrusts and head shaking, in evening eyes start jittering and roll up and he has to close them to refixate (nystagmus-like motion), usually in the context of illness	Intermittently has jerking movements of his eyes usually in the context of illness	Retinitis pigmentosa	Bilateral retinal degeneration and optic atrophy	N/A
Other					
Mitochondrial/Electron transport chain analysis	N/A	Mitochondrial DNA whole genome sequencing was performed, no deleterious mutations were detected; muscle was sent to Baylor College of Medicine Mitochondrial Laboratory and electron transport chain testing showed no specific deficiencies	No deletions or duplications (done 2004)	N/A	N/A
Biochemical testing performed	N/A	Extensive metabolic evaluations have been unrevealing and included normal carbohydrate-deficient transferrins with no evidence of a CDG, normal alpha fetoprotein, normal ammonia, normal creatine kinase, normal hexosaminidase A, normal biotinidase, normal coenzyme Q10 quantification, normal plasma and CSF amino acids, normal 7-OH hydrocholesterol, normal peroxisomal panel, normal urine amino acids and organic acids, normal oligosaccharide screen, normal acylglycines and glycosaminoglycans, normal urine purine and pyrimidine	Carnitine T&F, acylcarnitine, CDG, MMA, UOA, PAA, lactate, biotin, peroxisomal studies	Very long-chain fatty acids for perioxisomal disorders was negative; metabolic screen for metabolic disorders was unremarkable	Normal acylcarnitines, amino acids, and organic acids

(Continued)

Table 1 Continued.

	Case 1 ACO2	Case 2 ACO2	Case 3 ACO2	Case 4 ACO2	Case 5 ACO2
Gene altered		panel, and normal enzyme testing for Niemann-Pick disease			
Additional genetic findings		He has a normal karyotype, normal array CGH	He has had normal karyotype, normal array CGH, normal Prader-Willi/Angelman syndrome methylation, normal MECP2, FMR1, and KCNA1. He has had normal mtDNA sequencing and normal ataxia evaluation through Athena. This included normal analysis of SCA1, SCA2, SCA3, SCA6, SCA7, SCA8, SCA10, SCA17, DRPLA, FRDA1, SCA14, SETX, POLG1, SCA5, SIL1, TTPA, and KCNC3	Normal SNP, normal Rett sequencing, normal PWS/Angelman methylation	Chromosomal analysis showed normal 46,XY, male karyotype; two copies of SMN1 gene, exon 7 were detected ruling out spinal muscular atrophy (SMA)	N/A
Primary diagnostic hypotheses	Multiple-drug sensitivities, asthma, received monthly or bimonthly IVIg for suspected immune disorder may help control symptoms	At ~20 months of age he had a minor febrile illness during which time he became very ataxic and lost ability to walk or crawl; diagnosed with a viral illness and ataxia persisted for months with gradual recovery; history of regression and ataxia with illnesses and global developmental delay; receives monthly or bimonthly IVIg for suspected immune disorder which helps control infections and other symptoms	Mitochondrial disease (initially), SCA	SMA-like presentation, creatine kinase (CK) was normal (152 U/L); muscle biopsy revealed nonspecific myopathy and there was no evidence of congenital muscular dystrophy, nemaline myopathy, dystrophinopathy, or sarcoglycanopathy; merosin was normally expressed	Metabolic cerebral palsy

N/R, Not reported; N/A, Not assessed.

© 2020 The Authors. *Annals of Clinical and Translational Neurology* published by Wiley Periodicals LLC on behalf of American Neurological Association
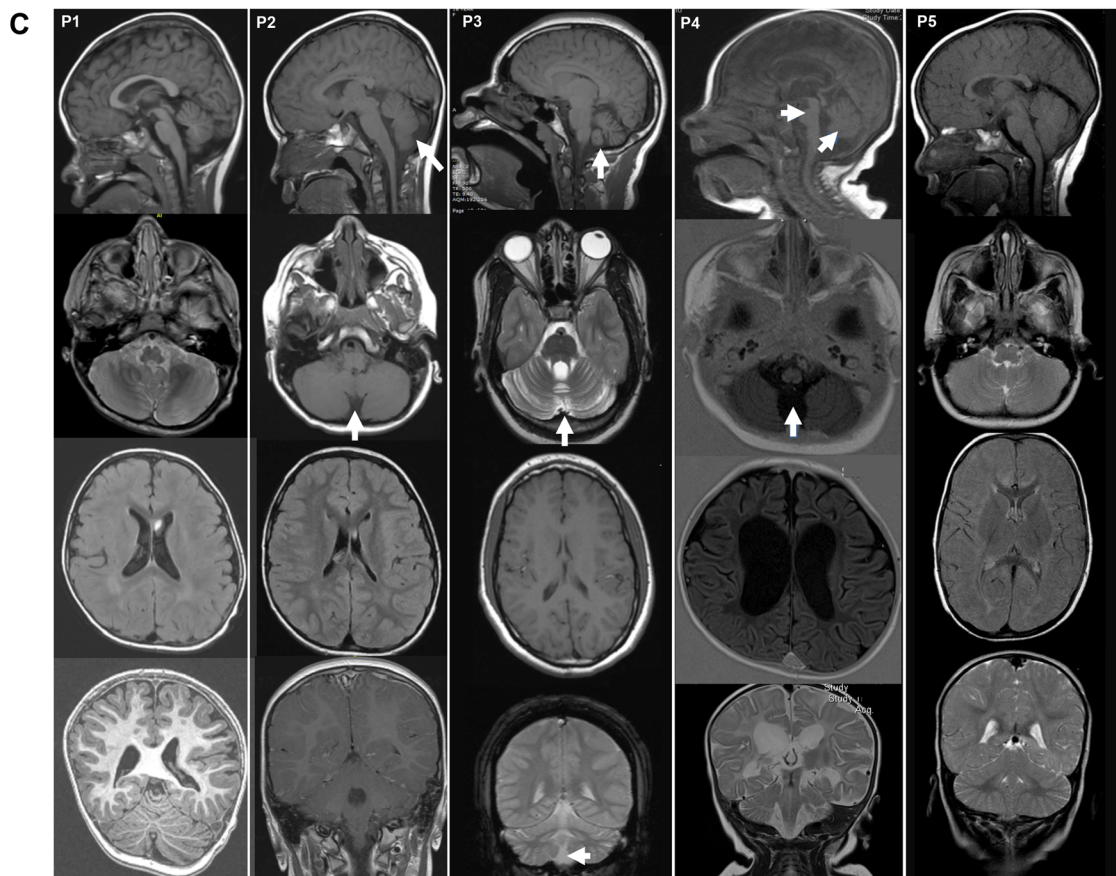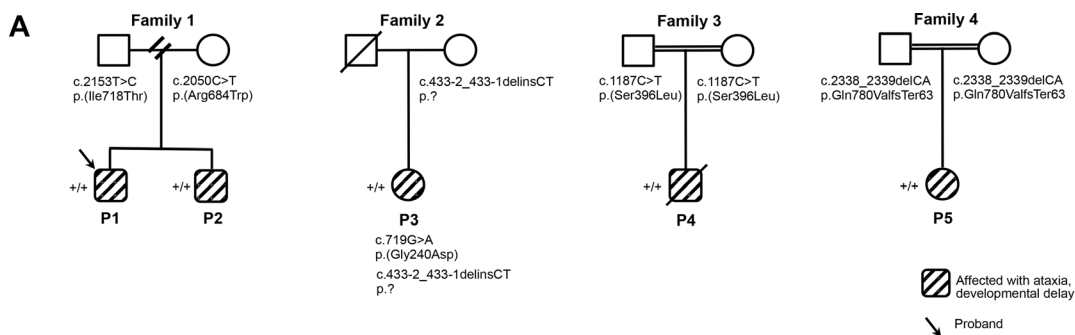
Figure 1. (A) Pedigrees of families 1–4 showing inheritance of disease-associated variants in *ACO2*. Standard pedigree symbols are used; squares, male; circles, female; slush through symbols, deceased individuals. Shading indicates affected status. An arrow indicates the proband in family 1. (B) Images of P1 and P2 (brothers), and P4. Images of P1 were taken at 9 years of age and at 12 years of age for P2. Images of P4 at the age of 8 months showing severe hypotonia. (C) Typical MRI findings in patients with ACO2-related disorders. Serial images of patients 1–5 (P1–P5) are shown top to bottom. Representative sagittal, two axial, and coronal images are shown for each patient. Noncontrast MRI of the brain of P1 was performed at 2 years and 3 months of age. MRI of the head was normal with normal myelination for age with bilateral terminal zones in the periatrial white matter. The pons and superior cerebellar vermis are slightly small for age. Brain MRI for P2 was performed at 6 years of age. Midbrain, pons, and middle cerebellar peduncles were noted to be small in size. MRI of the cerebellar hemispheres was normal, although the superior cerebellar vermis was felt to be mildly atrophic. In P3, brain MRI at 16 years of age showed mild cerebellar atrophy but was otherwise normal. In P4, brain MRI at 5 months and 11 days showed dilatation of the ventricles and prominent subarachnoid spaces, thinning of the corpus callosum, hypoplastic cerebellar vermis, and hypoplastic pons. Brain MRI in P5 was performed before 4 years of age and showed global hypomyelination and other nonspecific findings.

P3 is a 26-year-old female who presented with cerebellar hypoplasia, ataxia, spastic cerebral palsy, seizures, optic atrophy, and retinitis pigmentosa (Fig. 1A). This individual has moderate-to-severe intellectual disability, a vocabulary of 4–5 words, and is non-ambulatory.

P4 was delivered at term to a 27-year-old primigravida mother. His parents are first cousins (Fig. 1A). Antenatal follow up was unremarkable. He was admitted to neonatal intensive care unit (NICU) 2 h after birth because of cyanosis. He was noticed to have poor respiratory drive and respiratory acidosis. Neurologic examination showed generalized hypotonia with diminished reflexes. He developed abnormal episodes characterized by twisting movements involving his arms and seizure disorder that was controlled by clonazepam. An electroencephalographic study (EEG) revealed gross abnormalities consistent with multifocal epilepsy. He had absent visual tracking and protective blinking. Ophthalmologic examination showed bilateral retinal degeneration and optic atrophy. He was overall nondysmorphic (Fig. 1B). Cardiovascular workup was normal. He had central apnea requiring ventilator support and failed several attempts of weaning and extubation until his death at the age of 9 months.

P5 is an 11-year-old female with progressive spastic quadriplegia, severe hypotonia, absent visually evoked potentials, and severe developmental and motor delays (Fig. 1A). She was born at term following an uneventful pregnancy via spontaneous vaginal delivery. She had her first recognized seizure at 3 months of age and has had at least one seizure per week since then despite being on three antiepileptic medications (Levetiracetam, topiramate, and lamotrigine).

Additional details can be found in the supplemental materials and in Table 1.

Laboratory investigations

P1 had a normal karyotype and normal array CGH testing. His older brother (P2) had more extensive evaluations including a normal karyotype, normal array CGH, normal Prader-Willi/Angelman syndrome methylation testing, and normal *MECP2*, *FMR1*, and *KCNA1* gene

testing. Extensive metabolic evaluations were unrevealing as well. These included normal ammonia, creatine kinase, carbohydrate-deficient transferrin, alpha fetoprotein, hexosaminidase A, biotinidase, coenzyme Q10 quantification, amino acids (plasma, CSF, urine), 7-dehydrocholesterol, peroxisomal panel, urine amino acids, oligosaccharide screen, acylglycines, glycosaminoglycans, urine purine and pyrimidine panel, hexosaminidase A, biotinidase, sphingomyelinase, and mitochondrial respiratory chain complex probe. He also had normal mitochondrial DNA (mtDNA) sequencing and normal ataxia evaluation through Athena Diagnostics. This included normal analyses of *SCA1*, *SCA2*, *SCA3*, *SCA6*, *SCA7*, *SCA8*, *SCA10*, *SCA17*, *DRPLA*, *FRDA1*, *SCA14*, *SETX*, *POLG1*, *SCA5*, *SIL1*, *TTPA*, and *KCNC3*.

P3 had a normal microarray, normal *MECP2* gene testing, normal PWS/Angelman methylation studies, and normal mitochondrial testing (including deletions/duplications). Biochemical testing including total and free carnitine, acylcarnitine profile, carbohydrate-deficient transferrin, urine organic acids, lactate, biotin, and peroxisomal studies were all normal.

P4 had normal 46, XY male karyotype. His creatine kinase was normal (152 U/L). Muscle biopsy revealed nonspecific myopathy and there was no evidence of congenital muscular dystrophy, nemaline myopathy, dystrophinopathy, or sarcoglycanopathy. Merosin was normally expressed. Testing for spinal muscular atrophy (SMA) was normal. Very long-chain fatty acids for peroxisomal disorders were negative. Additional metabolic screening was unremarkable.

A limited clinical history for P5 showed acylcarnitine testing, plasma amino acids, and urine organic acids were normal.

Additional details can be found in the supplemental materials and in Table 1.

Brain imaging

A comparison of brain MRI findings in each patient is shown in Figure 1C. P1 had noncontrast MRI of the

brain and lumbar spine, without comparison performed at 2 years and 3 months of age. MRI of the head was normal with normal myelination for age with bilateral terminal zones in the periatrial white matter. The pons and superior cerebellar vermis were slightly small for age (Fig. 1C). Lumbar spine, from T7 vertebral body through the sacrum showed a normal spinal cord, conus, and filum terminale without evidence of tethered cord (not shown). P2 had his most recent brain MRI at 6 years of age. Midbrain, pons, and middle cerebellar peduncles were noted to be small in size (Fig. 1C). MRI of the cerebellar hemispheres was normal, although the superior cerebellar vermis was felt to be mildly atrophic. There was mildly prominent T2 signal surrounding the 4th ventricle, but no unusual enhancement. The corpus callosum was within normal limits. In P3, brain MRI at 16 years of age showed mild cerebellar atrophy but was otherwise normal (Fig. 1C). A brain CT at age 18 revealed similar findings (not shown). In P4, brain MRI at 5 months and 11 days of age showed dilatation of the ventricles and prominent subarachnoid spaces, thinning of the corpus callosum, hypoplastic cerebellar vermis, and hypoplastic pons (Fig. 1C), while brain CT at the age of 1 day was unremarkable. Brain MRI in P5 was performed around 4 years of age and showed global hypomyelination and other nonspecific findings (Fig. 1C).

Genetic and in silico analysis

P1 and P2 both carry compound heterozygous variants, paternally inherited c.2153T>C: p.(Ile718Thr) and maternally inherited c.2050C>T: p.(Arg684Trp) (Fig. 2A and B). The p.(Ile718Thr) variant has not been reported previously, or has it been observed in population databases (gnomAD). The variant falls in a highly conserved residue (to yeast) and is predicted to be damaging by in silico prediction software. ΔΔG predictions (a measure of the change in monomeric protein stability when a point mutation is introduced) show a destabilizing effect of the p.(Ile718Thr)

variant (ΔΔG: −3.151 kcal/mol) with an increase in molecule flexibility (ΔΔSVib ENCoM: 0.275 kcal/mol/K) (Fig. 2C). The p.(Arg684Trp) variant was previously observed in two recently described patients *in trans* with the c.1787A>G: p.(His596Arg) missense variant.[7] Both residues are evolutionary conserved and were predicted to impact substrate binding. Functional studies in the Δaco1 yeast strain showed a 25% reduction in enzymatic activity for the homologous Arg684Trp variant, Arg681Trp, suggesting that Arg684Trp is a hypomorphic ACO2 variant.[7,18,19]

P3 was found to carry two variants, c.719G>A: p.(Gly240Asp) and c.433-2_433-1delinsCT in trans, with the c.433-2_433-1delinsCT splice-site mutation confirmed in the patient's mother (Fig. 2A and B). Her father was deceased at the time of testing. In silico splice prediction tools (SpliceSiteFinder-like, MaxEntScan, GeneSplicer, and NNSPLICE) show complete loss of the exon 4 splice acceptor site with the c.433-2_433-1delinsCT variant. The p.(Gly240Asp) variant has been reported rarely in gnomAD (0.000007953% or 2/251480 total alleles) and falls in a highly conserved residue (to yeast). ΔΔG predictions show a destabilizing effect of the p.(Gly240Asp) variant (ΔΔG: −0.057 kcal/mol) with a net decrease in molecule flexibility (ΔΔSVib ENCoM: −0.168 kcal/mol/K) (Fig. 2C).

In P4, the c.1187C>T: p.(Ser396Leu) homozygous variant falls in a moderately conserved residue and has not been reported in gnomAD or other population databases (Fig. 2A and B). In silico prediction algorithms consistently show a deleterious effect of this mutation and ΔΔG predictions show a stabilizing effect (ΔΔG: 1.519 kcal/mol) with a net decrease in molecule flexibility (ΔΔSVib ENCoM: −0.375 kcal/mol/K) (Fig. 2C). This novel variant falls near the c.1181G>A: p.(Gly394Glu) variant that has been observed in several patients including in association with infantile cerebellar-retinal degeneration in trans with a p.(Trp574Cys) variant.[18]

In P5, the c.2338_2339delCA: p.(Gln780ValfsTer63) homozygous variant falls in the last amino acid before the

Figure 2. (A) Schematic diagram of the ACO2 protein showing the mitochondrial aconitate hydratase catalytic and swivel domains. Patient variants are overlaid on the diagram and are color-coded based on their effect on the encoded protein (Based on NCBI Reference Sequences: NM_001098.2, NP_001089.1). Variants identified in patients described in this cohort are shaded orange. Protein diagrams were generated using ProteinPaint (https://proteinpaint.stjude.org/). (B) MTR-Viewer results for *ACO2*. The line graph displays the Missense Tolerance Ratio (MTR) distribution (measure of regional intolerance to missense variation) for *ACO2* with regions in red indicating observed variation significantly deviates from neutrality (http://biosig.unimelb.edu.au/mtr-viewer/). Missense mutations identified in the patient cohort are overlaid and shown as orange circles. (C) Visual representation of the change in vibrational entropy energy between wild-type (WT) and missense mutations (MUT) generated using DynaMut (http://biosig.unimelb.edu.au/dynamut/). Amino acids colored according to the vibrational entropy change upon mutation with blue indicating a rigidification of the protein structure and red indicating a gain in overall flexibility. A zoomed-in visualization of the predicted interatomic interactions for WT and MUT residues are shown as sticks and colored in light green along with surrounding residues which are involved in any type of interactions. A table summary of the predicted ΔΔG and ΔΔS predictions are shown below the models for each missense variant in *ACO2* (ΔΔG: negative values are destabilizing and positive values are stabilizing).
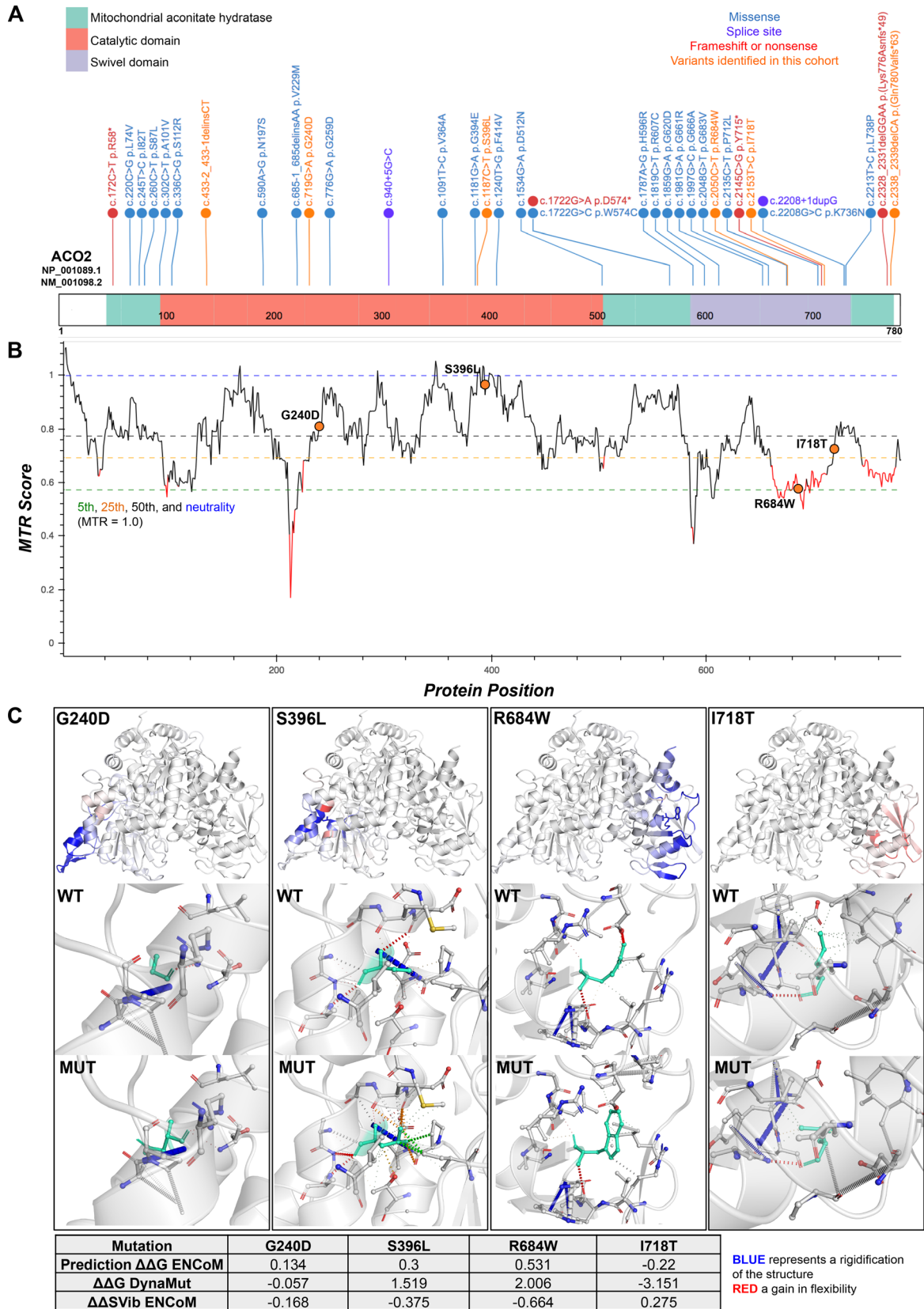
Table 2. Clinical characteristics of ACO2-deficient patients and associated functional studies of residual enzyme function.

Reference	Fukata	Metodiev	Metodiev	Metodiev	Metodiev	Metodiev	Bouwkamp
PMID	31106992	25351951	25351951	25351951	25351951	25351951	29577077
Gender	Female	Male	Male	Metodiev	Male	Female	Male
Ethnicity	Japanese	French	French	Algerian	Algerian	N/R	Arab-Bedouin
Age at report	Died at 5 years, pneumonia	36 years	41 years	Died 57 days	Died 61 days	4 y	28 y
OPA	Yes	Yes	Yes	Bilateral edema of optic disks	Extinguished VEP	Optic disk pallor, altered VEP	No; developed abnormal tracking as adult
Cerebellar atrophy	Yes	No	No	Moderate	Moderate	Moderate at 4 years	Mild
Peripheral neuropathy	N/A	No	No	N/A	N/A	N/A	No
ID	Yes	No	No	N/A	N/A	N/A	Yes
Ataxia	Yes	No	No	Yes	Yes	Yes	HSP
Epilepsy	Yes, controlled with medication	No	No	N/R	N/R	N/R	Yes (3 months); spontaneous remitted by 5 years
Communication	No communication	No	No	N/A	N/A	N/R	Vocalizations
Hypotonia	Yes	No	No	N/A	N/A	Yes	N/R
Microcephaly	Normal at birth, not mentioned subsequently	No	No	Normal at birth	Normal at birth	N/R	Yes (3rd percentile, adult)
Dysmorphic features	N/R			N/R	N/R	N/R	
Other		Reportedly isolated OPA	Reportedly isolated OPA	Metabolic acidosis, hyperglycemia, apneic episodes	Apneic episodes		Failure to thrive
Sensorineural hearing loss	Yes					No	No
Presentation	ICRD	Optic atrophy	Optic atrophy	ICRD with central apnea	ICRD with central apnea	Mild ICRD	HSP, infections, severe ID
Functional studies (patient level)							
Tissue source	Fibroblasts	Fibroblasts	Fibroblasts	Fibroblasts	Fibroblasts	Fibroblasts	Immortalized Leukocytes
Protein expression	36	20	20	100	N/P	20	20
Activity	15	60	66	<5	N/P	30	30
Substrate	Citrate	Cis aconitic acid	Cis aconitic acid	Cis aconitic acid	Cis aconitic acid	Cis aconitic acid	
ACO1 activity considered?	No	Yes, Citramalate	Yes, Citramalate	Yes, Citramalate ACO2 inhibition	Yes, Citramalate ACO2 inhibition	Yes, Citramalate ACO2 inhibition	Yes, fractionation
Mitochondrial depletion	N/P	N/P	N/P	N/P	N/P	N/P	
Mitochondrial respiration studies	N/P					Normal	Reduced
Notes							

Functional studies (variant level)

cDNA	c.1534G>A	c.1997G>C	c.220C>G	c.1981G>A	c.220C>G	c.1981G>A	c.776G>A	c.776G>A	c.2208G>C	c.2328_2331 delGAAG	c.1240T>G	Hmz
Protein	p.Asp512Asn	p.Gly666Ala	p.Leu74Val	p.Gly661Arg	p.Leu74Val	p.Gly661Arg	p.Gly259Asp	Hmz	p.Gly259Asp	Hmz	p.Lys736Asn	p.Lys776Asnfs*49	p.Phe414Val
Model	HEK293 cells											
Enzyme activity	76%	55%										
Complementation	N/P	N/P	No	Yes	No	Yes	No		No		No		No
Mitochondrial respiration											50% max respiration rate	
RT-PCR												

N/R, Not reported; N/A, Not assessed; N/P, Not performed; Hmz, Homozygous; HSP, Hereditary spastic paraplegia; ICRD, Infantile cerebellar retinal degeneration; OPA, Optic atrophy; VEP, Visual-evoked potential.

Bouwkamp	Marelli	Srivastava	Sadat	Sharkia	Speigel
29577077	29564393	28545339	26992325	30689204	22405087
Female	Female	Male	Male	Male	8 patients
Arab-Bedouin	Caucasian	N/R	Afro-Caribbean and East Indian	African/Caucasian	
14 y	56 y	18 y	3 years	8 and 6 years	0.5–18 years
No	Yes; older at evaluation	Yes	Appeared normal	N/A	Optic atrophy, strabismus, nystagmus
No	Mild	Mild	No prominent cerebellar involvement with oculomotor dyspraxia, truncal unsteadiness and disequilibrium, gait ataxia, mild limb dysmetria, and revealed prominent cerebellar involvement with oculomotor dyspraxia, truncal unsteadiness and disequilibrium, gait ataxia, mild limb dysmetria, and reduced muscle tone. Prominent cerebellar involvement with oculomotor dyspraxia, truncal No reduced muscle tone	Normal at 2 years	Severe
No	No	Yes	N/R		N/R
Moderate	Mild	Severe profound; partially spared cognition compared to ICRD cases	Yes	Moderate	Severe-profound
Episodic; incurrent febrile illness	Lower HSP, upper limb ataxia	Childhood-onset (15 months), initially with intercurrent illness then progressing to constant	Truncal ataxia (6 months)	1 year	1 year
No		Intractable	Myoclonic jerks during illness	Yes, 1 and 1.5 years	Yes (6/8)
Verbal		Full sentences; dysarthria		Verbal, delayed acquisition	Nonverbal
N/R		Axial hypotonia; appendicular hypertonia	Moderate	Yes, 1 year	Yes
Acquired; 3rd percentile		N/R		No	Yes
Bilateral 2,3 syndactyly of feet		N/R	Down slanting palpebral fissures, prominent forehead, and droopy eyelids		
Around 3 years recurrent encephalopathic episodes and regression	Motor delay 3 years	Retinal dystrophy, short stature (z-score − 4.75)	Cog-wheel eye saccades		
No		N/R	Yes		
HSP	OPA, HSP	Mild ICRD	Ataxia	Ataxia	ICRD
Immortalized Leukocytes	Fibroblasts	N/A	Fibroblasts		Lymphoblasts
100	50% full-length RNA transcript		Unchanged		N/A
20	50		20		11.9+/- 9.2% Controls
Yes, fractionation	Citrate Not described				N/A
	Not seen		Yes, 50% Reduction		
Reduced	Normal		Deficiency, 40% reduction in max respiratory rate		
		No functional studies	50% reduction in citrate synthase activity; Krebs cycle proteins were elevated in expression suggesting possible compensatory mechanism		
c.1240T>G Hmz	c.2135C>T	c.940 + 5G>C c.2328_2331 delGGAA	c.1091T>C c.2135C>T c.1819C>T	c.1787A>G c.2050C>T	c.336C>G Hmz
p.Phe414Val	p.Pro712Leu	Frameshift	p.Val364Ala p.Pro712Leu p.Arg607Cys	p.Arg684Trp ACO2, p.Arg681Trp aco1 p.His596Arg ACO2, p.His593Arg aco1	p.Ser112Arg
		N/A	N/P N/P Yeast Complementation	75% of controls 45% of controls	
No	N/P	N/P		No change Reduced; 45% of controls	No
		Smaller RNA product noted at about 50%			

TGA stop codon (Fig. 2A) and is a predicted stop loss alteration resulting in inclusion of a novel peptide sequence (VRAVPPRPAAGVKFSSTCAISGS DPSSHGFLF QDGVTRHASCSPLSPRSDCGCGGGVLKITF*) that is 62 amino acids in length. It is possible that this novel peptide could impair localization of this protein, lead to aggregation, or disrupt normal protein structure, thereby affecting overall stability. The same homozygous p.(Gln780ValfsTer63) variant was found in another Arab family (Family 046) in two affected children (phenotype similar to reported).[3,21] In addition, two other cases have been described with a similar frameshift mutation, c.2328_2331delGGAA: p.(Lys776Asnfs*49) that is also predicted to lead to the addition of a novel peptide sequence at the end of ACO2.[4]

Discussion

The five patients reported here demonstrate and expand the clinical heterogeneity associated with this disorder. The two sibling cases (P1 and P2) are unique in their mild and episodic disease presentation, while P3 and P5 are consistent with initial descriptions of the cerebellar-retinal form of disease. Only one other case has been reported with a mild presentation that included ataxia, hypotonia, occasional myoclonic jerks during times of illness, mild-to-moderate hearing loss bilaterally, but with no evidence of cerebellar atrophy or significant optic nerve involvement on MRI,[7] findings that were similarly absent in the two brothers. In addition, we describe a severe case (P4) with SMA-like presentation and early lethality due to respiratory failure. P4 presented with a severe form of cerebellar-retinal degeneration with ponto-cerebellar-retinal degeneration.

Two mildly affected patients were recently described in Sharkia et al. with compound heterozygous variants: c.1787A>G:p.(His596Arg) and c.2050C>T:p.(Arg684Trp). Functional testing of the p.R684W and p.H596R variants showed a ~25% and 55% reduction in activity compared to wild type in a yeast model, suggesting that they represent hypomorphic variants with intermediate activities.[7] Patient E2 was an 11-year-old male who requires support while walking, and has severe dysarthria which manifested at 2 years of age with febrile seizures.[7] This individual experienced episodes of polymyoclonus lasting from 12 to 24 hours and involving limbs, abdomen, and facial muscles with further worsening of ataxia at 4 years of age.[7] He had only moderate cognitive delays and MRI show signs of mild progressive cerebellar atrophy.[7] His brother (Patient E3) was 9 years of age and uniquely presented at 3 years with a sleep disorder.[7] He developed a pervasive behavioral disorder following a single episode of tremor and polymyoclonus at 18 months of age.[7] Brain MRI was normal at age 4 and reportedly showed some mild cerebellar atrophy by age 6. These two patients show some similarities to P1 and P2 in our study, who were also found to carry the c.2050C>T:p.(Arg684Trp) variant in addition to a previously unreported 2153T>C: p.(Ile718Thr) variant.[7] Given the mild clinical presentations in both families sharing the p.R684W and supportive functional evidence from Sharkia et al. showing only minor reductions in ACO2 activity, it is highly likely that this and other hypomorphic variants will be identified in patients without classic ICRD.

Enzyme activity of ACO2 in patient tissues or variant-specific assays in vitro has been utilized to evaluate variant pathogenicity and has been suggested to correlate with phenotype.[7] Differences in in vitro enzyme testing methodologies between studies, including use of different substrates or methods to distinguish ACO2 from ACO1 activity, complicate evaluation of the measured enzyme activity and its association with clinical phenotype (Table 2). In a limited number of total cases, patients with variants that result in reduced expression of a largely functional ACO2 enzyme result in milder phenotypes than variants resulting in greatly reduced activity (Table 2). The lowest enzyme activity described, ~5% in a patient who died at 57 days, is still comparably greater than the inhibition threshold for other enzymopathies, such as lysosomal storage diseases (Table 2). ACO2 threshold effects may be apparent during times of intercurrent illness when some patients have demonstrated worsening ataxia.[3,5,7]

Several studies now demonstrate *ACO2* variants can result in overall reduction in the max respiratory rate by O_2 consumption rate testing (Table 2).[3,5,7] A single report of a 3-year-old with compound heterozygous alterations in *ACO2* demonstrated mitochondrial DNA depletion of 50% compared with controls, raising the possibility that ACO2 deficiency may impair mitochondrial maintenance (Table 2).[4] In yeast, aconitase (aco1) has been shown to be important in mtDNA maintenance and this function is independent of the enzymatic role of aco1.[1] Mitochondrial depletion has not been examined in all cases thus far and may provide an explanation for inconsistencies between the degree of residual enzyme activity and the observed phenotypic severity (Table 2).

Metabolite testing has not revealed a diagnostic pattern on traditional biochemical tests, including urine organic acid and plasma amino acid profiles.[2] Abela et al. studied plasma metabolites from patients with *ACO2* variants and identified a putative metabolic signature focusing primarily on patients with an ICRD phenotype.[22] This pattern was seen in an aggregate analysis, leaving individual patient sensitivity and specificity to be determined. It may stand that measurement of Krebs cycle intermediates in plasma may

add clinical value in cases with *ACO2* variants, since these metabolites are not perturbed in urine.[2,7]

In summary, these five new cases significantly expand the mutational and clinical spectrum associated with this disorder. Importantly we propose that hypomorphic variants may be associated with a more mild disease presentation and may manifest primarily in the context of febrile illness. Many patients have been reported to develop episodic worsening of ataxia or other clinical features in the setting of febrile illness. Both P1 and P2 were initially suspected to have an immunodeficiency disorder and have been treated with monthly IVIg for several years, which may have helped control their ataxia and other symptoms. With further study, IVIg may represent a possible supportive therapy for some patients that reduces the frequency of infections, which have been reported to worsen clinical symptoms in some patients. Given our combined findings, we propose unifying the diverse clinical presentations under the collective term, ACO2-related disorders. Additionally, it is important to recognize milder forms of the disorder, which may escape detection due to atypical disease presentation and may be amenable to supportive therapies.

Acknowledgments

Conflict of Interest

The authors declare no conflicts of interest.

References

1. Chen XJ, Wang X, Kaufman BA, Butow RA. Aconitase couples metabolic regulation to mitochondrial DNA maintenance. Science 2005;307:714–717.

2. Spiegel R, Pines O, Ta-Shma A, et al. Infantile cerebellar-retinal degeneration associated with a mutation in mitochondrial aconitase, ACO2. Am J Hum Genet 2012;90:518–523.

3. Srivastava S, Gubbels CS, Dies K, et al. Increased survival and partly preserved cognition in a patient with ACO2–related disease secondary to a novel variant. J Child Neurol 2017;32:840–845.

4. Sadat R, Barca E, Masand R, et al. Functional cellular analyses reveal energy metabolism defect and mitochondrial DNA depletion in a case of mitochondrial aconitase deficiency. Mol Genet Metab 2016;118:28–34.

5. Bouwkamp CG, Afawi Z, Fattal-Valevski A, et al. ACO2 homozygous missense mutation associated with complicated hereditary spastic paraplegia. Neurol Genet 2018;4:e223.

6. Marelli C, Hamel C, Quiles M, et al. ACO2 mutations: a novel phenotype associating severe optic atrophy and spastic paraplegia. Neurol Genet 2018;4:e225.

7. Sharkia R, Wierenga KJ, Kessel A, et al. Clinical, radiological, and genetic characteristics of 16 patients with ACO2 gene defects: delineation of an emerging neurometabolic syndrome. J Inherit Metab Dis 2019;42:264–275.

8. Monies D, Abouelhoda M, Assoum M, et al. Lessons learned from large-scale, first-tier clinical exome sequencing in a highly consanguineous population. Am J Hum Genet 2019;104:1182–1201.

9. Sobreira N, Schiettecatte F, Valle D, Hamosh A. GeneMatcher: a matching tool for connecting investigators with an interest in the same gene. Hum Mutat 2015;36:928–930.

10. Bhoj EJ, Li D, Harr M, et al. Mutations in TBCK, encoding TBC1-domain-containing kinase, lead to a recognizable syndrome of intellectual disability and hypotonia. Am J Hum Genet 2016;98:782–788.

11. Monies D, Abouelhoda M, AlSayed M, et al. The landscape of genetic diseases in Saudi Arabia based on the first 1000 diagnostic panels and exomes. Hum Genet 2017;136:921–939.

12. Du J, Sudarsanam M, Pérez-Palma E, et al. Variant score ranker – a web application for intuitive missense variant prioritization. Bioinformatics 2019;35:4478–4479.

13. Bienert S, Waterhouse A, de Beer TAP, et al. The SWISS-MODEL repository-new features and functionality. Nucleic Acids Res 2017;45(D1):D313–D319.

14. Rodrigues CH, Pires DE, Ascher DB. DynaMut: predicting the impact of mutations on protein conformation, flexibility and stability. Nucleic Acids Res 2018;46(W1):W350–W355.

15. Karczewski KJ, Francioli LC, Tiao G, Cummings BB. Variation across 141,456 human exomes and genomes reveals the spectrum of loss-of-function intolerance across human protein-coding genes. BioRxiv 2019;DOI:https://doi.org/10.1101/531210

16. Silk M, Petrovski S, Ascher DB. MTR-Viewer: identifying regions within genes under purifying selection. Nucleic Acids Res 2019;47(W1):W121–W126.

17. Zhou X, Edmonson MN, Wilkinson MR, et al. Exploring genomic alteration in pediatric cancer using ProteinPaint. Nat Genet 2016;48:4–6.

18. Helbig KL, Farwell Hagman KD, Shinde DN, et al. Diagnostic exome sequencing provides a molecular diagnosis for a significant proportion of patients with epilepsy. Genet Med 2016;18:898–905.

19. Farwell KD, Shahmirzadi L, El-Khechen D, et al. Enhanced utility of family-centered diagnostic exome sequencing with inheritance model-based analysis: results from 500 unselected families with undiagnosed genetic conditions. Genet Med 2015;17:578–586.

20. Charng W-L, Karaca E, Coban Akdemir Z, et al. Exome sequencing in mostly consanguineous Arab families with neurologic disease provides a high potential molecular diagnosis rate. BMC Med Genomics 2016;9:42.

21. Metodiev MD, Gerber S, Hubert L, et al. Mutations in the tricarboxylic acid cycle enzyme, aconitase 2, cause either isolated or syndromic optic neuropathy with encephalopathy and cerebellar atrophy. J Med Genet 2014;51:834–838.

22. Abela L, Spiegel R, Crowther LM, et al. Plasma metabolomics reveals a diagnostic metabolic fingerprint for mitochondrial aconitase (ACO2) deficiency. PLoS ONE 2017;12:e0176363.

Supporting Information

Additional supporting information may be found online in the Supporting Information section at the end of the article.

Figure S1. Visual representation of the change in vibrational entropy energy between all wild-type (WT) and missense *ACO2* mutations (MUT) described to date. Simulations were performed using a homology model (PDB: 1b0j.1.A) of human mitochondrial aconitate hydratase (Q99798) from the SWISS-MODEL Repository (SMR) and generated by the SWISS-MODEL homology modeling pipeline.

Figure S2. A zoomed-in visualization of the predicted interatomic interactions for WT and MUT residues for all missense *ACO2* variants described to date. WT and MUT residues are shown as sticks and colored in light green along with surrounding residues which are involved in any type of interactions.

Table S1. List of all variants in *ACO2* and associated clinical phenotypes, population frequency, and in silico predictions for pathogenicity.

Table S2. A table summary of the predicted variation in free energy ($\Delta\Delta G$) and vibrational entropy ($\Delta\Delta S$) is shown for each missense variant in *ACO2* described to date.

Data S1. Description of supplementary materials and methods with supplemental references.